Highly Sensitive Plasmonic Silver Nanorods

Arpad Jakab,[†] Christina Rosman,[†] Yuriy Khalavka,[†] Jan Becker,[†] Andreas Trügler,[‡] Ulrich Hohenester,[‡] and Carsten Sönnichsen[†,*]

[†]MAINZ Graduate School of Excellence and Institute of Physical Chemistry, University of Mainz, Jakob-Welder-Weg 11, 55128 Mainz, Germany, and [‡]Institute of Physics, Karl-Franzens University Graz, Universitätsplatz 5, 8010 Graz, Austria

Sensor devices based on the refractive index sensitivity of surface plasmons have emerged on the market in the past decade. Attempts to increase the sensitivity and reduce the sensor size focus on single particle-based sensors supporting localized surface plasmons polaritons (*LSPP*) or particle plasmons.[1−3] As recently reported, single-particle sensors can have a higher sensitivity than propagating surface plasmon-based sensors.[4]

The spectral position of the localized surface plasmon is highly dependent on the dielectric properties of the surrounding medium.[5] For example, a change of the surrounding refractive index of 0.02 from 1.333 to 1.353 results in a red shift of the resonance wavelength by 5.1 nm for a gold NRs (nanorods) with an aspect ratio of 2.5. For optimal sensing of the smallest dielectric changes (*i.e.*, binding of small molecules), the spectral shift of the resonance wavelength upon changing the surrounding medium has to be maximized. Increasing the spectral shift can be achieved by various methods such as optimizing the shape and size,[6−9] interparticle distance,[10,11] or the material of the particle.[9,12] In recent times, efforts have been intensified to investigate silver nanoparticle sensitivity.[13,14] Silver and gold nanotriangle sensitivities of self-assembled monolayers have been reported earlier,[15] but because of different monolayer thicknesses the differing sensitivities could not be attributed to optical properties of the metals. In this work, we present experimental results of single silver nanorod and gold nanorod sensitivities revealing that silver nanorods have a higher sensitivity than gold nanorods at the same resonance wavelength and that, contrary to earlier predictions,[16] the background polarizability of the d-band electrons strongly influences the sensitivity. We provide a theoretical discussion of the differing sensitivities based on medium long wavelength

ABSTRACT We compare the single-particle plasmonic sensitivity of silver and gold nanorods with similar resonance wavelengths by monitoring the plasmon resonance shift upon changing the environment from water to 12.5% sucrose solution. We find that silver nanoparticles have 1.2 to 2 times higher sensitivity than gold, in good agreement with simulations based on the boundary-elements-method (BEM). To exclude the effect of particle volume on sensitivity, we test gold rods with increasing particle width at a given resonance wavelength. Using the Drude-model of optical properties of metals together with the quasi-static approximation (QSA) for localized surface plasmons, we show that the dominant contribution to higher sensitivity of silver is the lower background polarizability of the d-band electrons and provide a simple formula for the sensitivity. We improve the reversibility of the silver nanorod sensors upon repeated cycles of environmental changes by blocking the high energy parts of the illumination light.

KEYWORDS: silver · gold · nanoparticle spectroscopy · plasmon · sensitivity · reshaping · reversibility · morphology

approximation (MLWA)[5,17] to account for size dependent effects. Simplification with the quasi-static approximation (QSA) leads to an elegant formulation of sensitivity as function of resonance wavelength position, plasmonic material parameters, and the refractive index of the embedding medium.

DISCUSSION

Synthesis. For our study, we form silver nanorods with various aspect ratios in solution adapting a two-step "seeded growth" approach developed by Kitaev *et al.*[18] with small modifications in illumination and heating. In the first step, faceted silver "seeds" are produced under light illumination. We use a blue LED lamp (141mW, peak maximum @ 459.5 nm, full-width-at-half-maximum (fwhm) 20.53 nm) instead of the high power metal halide lamp used by Kitaev and co-workers. In the second step, the seeds are added to a "growth solution" where they develop into silver nanorods. We preheat the growth solution in a commercial microwave at 90 W for 1 min. Then $AgNO_3$ is added and the solution is placed into the microwave again for heating between 2 and
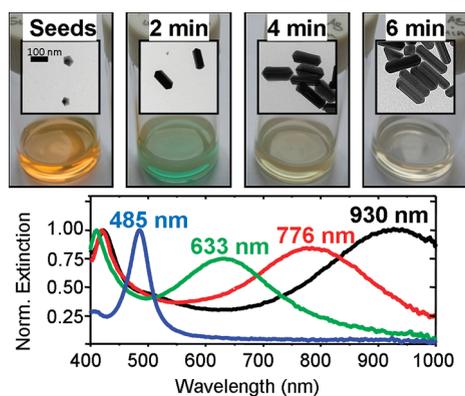
Figure 1. Representative silver nanorod samples are shown as photographs and TEM images together with the corresponding ensemble extinction spectra (bottom). The samples correspond to Ag-seeds and Ag-nanorods grown with 2, 4, and 6 min of heating time (from left to right). Their plasmon peak increases from 485 to 633, 776, and 930 nm.
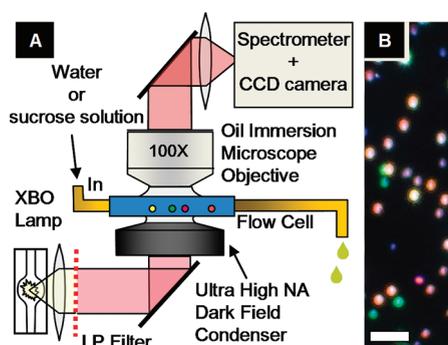

Figure 2. (A) Experimental wet environment dark-field set-up designed for single nanoparticle spectroscopy in various surrounding media. (B) Typical dark-field image of the nanoparticles; the scale bar is 10 μm.

6 min resulting in rods with increasing aspect ratio (AR). Heating for 2 min results in rods with an aspect ratio of 2.4 ± 0.8, heating for 4 min yields an aspect ratio of 2.9 ± 1.3, and heating for 6 min yields an aspect ratio of 4.0 ± 1.6. (Figure 1, top). We compare the plasmonic sensitivity of those silver rods with two types of gold nanorods with different widths. The nanorods with small widths were synthesized by the method of Nikoobakht et al.,[19] the ones with the large widths by the method of Ni et al.[20] The large nanorods have the advantage that their widths are comparable with the silver nanorods.

Plasmonic Nanorod Sensitivity. We observe the light scattering spectra of the single nanoparticles with a scanning dark-field setup[21] that allows for a rapid measurement of a large number of immobilized nanoparticles (Figure 2A). To measure the plasmon resonance shift upon changes in the refractive index of the environment (single-particle sensitivity), the nanoparticles are immobilized in a flat glass capillary or flow cell (the flow-cell preparation is described in detail in the Methods section).

To immobilize nanoparticles in the flow cell, we add a suspension of nanoparticles in water followed by a salt solution. The concentration of nanoparticles is

TABLE 1. Properties of the Silver and Gold Nanorods Used in Our Study (Sizes from TEM Images)

nanorod material	longitudinal ensemble		aspect ratio
	peak (nm)	width (nm)	(length/width)
Ag	633	55 ± 10	2.4 ± 0.7
Ag	776	59 ± 14	2.9 ± 1
Au	634	28 ± 4	2.0 ± 0.5
Au	702	18 ± 2	2.7 ± 0.52
Au	816	11 ± 2	4.1 ± 1.43
Au	680	50 ± 6	2.1 ± 0.5

adjusted by dilution to create a nanoparticle density in the field-of-view that allows the distinction of single particles (Figure 2B); that is, an average interparticle distance of about 10 μm. The addition of salt screens the surface charges that stabilize the nanoparticle suspension, which leads to nonspecific adsorption of nanoparticles to the glass surface of the flow cell. For gold nanorods, we used 0.1 M NaCl, for silver 0.1 M KNO$_3$ because, as discussed later, chloride ions can cause structural changes to silver nanoparticles.[22] To avoid aggregation, both liquids are separated in the source tube by a tiny air bubble that gets trapped in the entrance chamber of the flow cell, thus the mixing takes only place in the flow cell.

Table 1 summarizes the size characteristics of the nanorods used for single-particle spectroscopic measurements. We used only silver nanorods from samples with mean longitudinal plasmon resonances of 633 and 776 nm (green and red curves in Figure 1). Those silver nanorods had a mean width of about 55−60 nm and aspect ratios of 2.4 and 2.9, respectively. In comparison, the small gold nanorods have widths of 11−28 nm but with comparable aspect ratios, and the large gold nanorods have widths of 50 nm. More details about the nanoparticle size distribution are presented in Figure S1, Figure S2, Figure S3, Table S1 and Table S2 in the Supporting Information.

Sensitivity Measurements. The plasmon sensitivity quantifies the dependence of the plasmon resonance wavelength or frequency on changes in the dielectric properties of the surrounding medium. Sensitivity S (in wavelength units) is therefore defined by $S = d\lambda_{res}/dn$, where λ_{res} is the plasmon resonance wavelength and n is the refractive index of the surrounding medium. There are more elaborate measures to quantify the sensor quality of nanoparticles taking into account more realistic sensor concepts, for example FOM,[23,24] FOM*.[6] All of these quantities depend on the plasmon sensitivity. Here we focus on the sensitivity in wavelength units and refer to this term simply as "sensitivity".

We determined the plasmonic sensitivity experimentally by recording spectra of single immobilized nanoparticles in the initial environment (pure water, $n_1 = 1.3330$), then immersed in 12.5% sucrose solution ($n_2 = 1.3454$), and at the end again in water. The resulting experimental results are shown in Figure 3 (top panel).
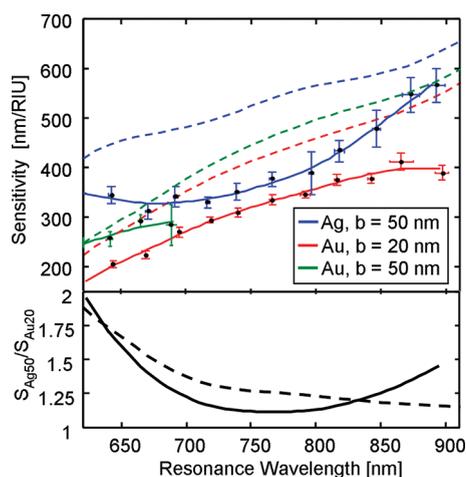
Figure 3. (Top) Experimental results (continuous lines) and BEM-simulation without substrate (dashed lines) of single-particle sensitivity of silver (blue line), 20 nm thick (red line), and 50 nm thick (green line) nanorods. The error bars indicate the uncertainty of the mean in a range of 25 nm. (Bottom) The experimentally obtained (continuous line) and BEM-simulated (dashed line) sensitivity enhancement (S_{Ag}/S_{Au}) of silver nanorods with 50 nm thickness in relation to gold nanorods with 20 nm thickness.

The experimentally obtained trend-lines (continuous lines) qualitatively follow the trend simulated with the boundary-element-method (BEM)[25] (dashed lines) but are lower than the simulation. However, the simulation was performed with a homogeneous medium around the particles, whereas in the experiment, the particles are attached to a glass substrate reducing the influence of the change in medium. The fact that the experimental silver trend shows a stronger deviation from simulations than the gold nanorods might be caused by additional damping of the plasmon resonance due to their penta-twinned crystal structure.[26]

We find that silver sensitivity is generally higher than gold sensitivity, thick gold nanorods have a higher sensitivity than the thinner gold nanorods, and in all cases, sensitivity depends on resonance wavelength. The sensitivity of silver nanorods reaches values above 400 nm/RIU, which is, up to now, the largest value for rodlike objects in this wavelength range.[8] Especially in the wavelength range of 600–700 nm, where thin gold nanorods have only a sensitivity of *ca.* 170 nm/RIU and thick gold nanorods of 250 nm/RIU, silver outperforms all gold nanorods with sensitivities around 340 nm/RIU.

To directly compare the sensitivity of the thin gold and silver nanorods over the entire measured spectral range, we show the ratio of their sensitivity (the sensitivity enhancement of silver compared to gold S_{Ag}/S_{Au}) in the bottom panel of Figure 3, both for the experimental data and the simulation. In simulations, we use 20 nm diameter for the thin gold NRs which is the average of the thicknesses of the thin gold NRs (11 to 28 nm) used in our experiments. Experiment and simulation agree well up to 850 nm in this diagram; the substrate effect effectively cancels out. At shorter wave-

lengths, around 620 nm, the enhancement reaches a factor of 2, at longer wavelengths the enhancement drops to a value between 1.1 and 1.2 with a slow increase above 850 nm that is not followed by the simulated results.

Discussion and Model. To understand the origin of the higher plasmonic sensitivity of silver compared to gold nanorods, we calculated sensitivities using simplified approaches, the medium long wavelength approximation MLWA and the quasi-static approximation (QSA).[5] MLWA includes size-dependent effects in plasmon resonance calculations, allowing us to investigate the impacts of particle size. In both cases, we use a simple Drude-type model for the dielectric function for gold and silver that separates the contribution of free and d-band electrons.

Whereas the boundary elements method (BEM) mentioned above provides exact solutions of the Maxwell equations (if the number of elements is sufficiently high), it provides little insight into the underlying physics. To understand the origin of the higher plasmonic sensitivity of silver compared to gold nanorods, it is instructive to use the quasi-static approximation to calculate the scattering cross section together with a simple Drude-type model for the dielectric function for gold and silver. Within those two approximations, the sensitivity S at a given resonance wavelength λ is given by the following equation (see Supporting Information for details):

$$S(\lambda) = \frac{\lambda}{n}\left(1 - \frac{\lambda_p^2}{\lambda^2}n_\infty^2\right)$$

where $\lambda_p = 2\pi c_0/\omega_p$ is the bulk plasmon wavelength ($\lambda_p = 136$ nm for gold and silver), $n_\infty = (\varepsilon_\infty)^{1/2}$ is the background refractive index (square root of the background dielectric constant) from the polarizability of the d-band electrons ($\varepsilon_{\infty,Au} = 9.84$ for gold and $\varepsilon_{\infty,Ag} = 3.7$ for silver correspond to $n_{\infty,Au} = 3.1$ and $n_{\infty,Ag} = 1.9$, respectively), and n is the refractive index of the surrounding medium. The equation above reveals that, contrary to earlier reports,[16] the sensitivity depends on the material through the strong difference in the background polarizability ε_∞ of gold and silver (the sensitivity decreases with increasing ε_∞ or n_∞). Despite the simplifications of the quasi-static approach and the Drude model for the dielectric function, the equation above predicts the sensitivity of nanorods remarkably well. Additional calculations using the medium long wavelength approximation (MLWA) that includes size effects, show that the above result is not drastically changed if radiation damping and retardation are taken into account. At a given wavelength, particle size influences plasmon sensitivity much less than the material (see Figure S10 in the Supporting Information).

Interestingly, all geometry related factors cancel out in the simple equation for the sensitivity shown above. Consequently, for small thickness/wavelength ratios (QSA) the sensitivity of a plasmonic nanorod at a given resonance wavelength is independent from its size and shape, and the formula could be valid more generally
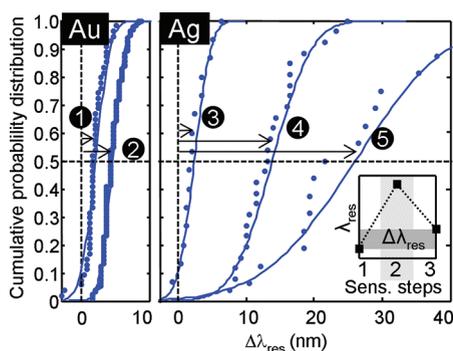
Figure 4. Cumulative distribution of single nanoparticle resonance wavelength shifts after one sensing measurement cycle (the sensing cycle shift). The continuous lines are Gaussian fits, the arrow indicates the mean cycle shift. Left graph: (1) small Au rods with 610 nm long pass (LP) filter (2) small Au rods without LP filter. Right graph: (3) Ag rods with 610 nm LP filter, (4) Ag rods with 530 nm LP filter, (5) Ag rods without LP filter. Inset at bottom right: definition of sensing cycle shift $\Delta\lambda_{res}$ in the cycle $n_1 \rightarrow n_2 \rightarrow n_1$.

for metal structures of other shapes. Our results are in accordance with the findings of Miller *et al*. that within the QSA the sensitivity of gold nanodiscs, nanocylinders, and nanoshells depends only on the location of the plasmon resonance peak and the dielectric properties of the involved materials.[27]

Sensing Reversibility. Whereas sensitivity alone seems to favor silver over gold, another important aspect for sensors is the *sensing reversibility* upon repeated changes of the environment. Given the fact that silver is less noble than gold, we carefully checked the reversibility. For this purpose, our measurements always went back to the initial environment at the end and we recorded the difference in resonance wavelength between initial and final resonance wavelength, a quantity we call the *sensing cycle shift*. For a reliable sensor, the mean sensing cycle shift should remain close to the experimental uncertainty (± 0.5 nm), and we disregarded all particles that did not show a full reversibility in the data sets for estimating particle sensitivity (reversibility within one standard deviation). Halide ions (Cl^- and especially Br^-) induce a reshaping of silver nanoparticles above a threshold concentration of $\sim 10^{-8}$ M, so we took care to avoid any use of those ions.[22,28,22,29] Generally, we found that even without halide ions present, silver nanoparticles showed much worse reversibility performance than gold. Light is known to modify silver nanoparticles.[22,30] We therefore suspected a light induced process, so we measured the reversibility with different filters in the light path.

In Figure 4 we show the sensing cycle shift of single nanorods plotted as a cumulative distribution

probability (an integrated histogram that allows an easy visualization of the mean value) measured under different illumination conditions where each dot corresponds to the sensitivity cycle shift of a single particle. The sensing cycle shift is decreasing with increasing cutoff wavelength of the long pass filter. The mechanism of this light-induced irreversible shift remains unclear and is probably a combination of heating[31,32] due to the absorbed light, (we believe that heat probably changes the arrangement of the crystalline domains in the pentatwinned silver nanorods) and photoetching.[22] The shift has nothing to do with changing the environment as we checked in experiments that show a red shift of nanoparticles monitored continuously in water (Figure S9 in the Supporting Information). Our experiments indicate that a sufficiently adjusted long pass filter allows the use of silver nanoparticles for sensing in environments without halide ions. However, these silver NRs are less suitable for other measures of plasmonic sensor performance like the "figure of merit" (FOM) due to the relatively large line width of our silver NRs (Supporting Information, Figure S8). We believe that the reduced radiation damping of silver NRs with a smaller volume could provide a substantially better performance for FOM sensitivity.

CONCLUSION

We have presented experimental results of silver nanorod sensitivity and compared them to results found for gold nanorods. Silver nanorods have up to two times higher sensitivity than gold nanorods in the spectral range of 600–700 nm. Increasing nanorod width leads to higher sensitivity but the dominant factor that influences the sensitivity is the material of the nanorods. In the region of 700–900 nm, the sensitivity is still about 10 to 20% higher. Calculations using MLWA (medium long wavelength approximation) and simulations with BEM (boundary element methods) confirm both material and size dependency. From simple theoretical arguments (Drude's model of optical properties of metals and the quasi-static-approximation QSA), we developed an expression for the sensitivity, and we could identify the lower background (d-band electron) polarizability of silver compared to gold as the main reason for the higher sensitivity. The reversibility of silver nanorod-based sensors is, generally, worse than gold nanorod-based sensors, but adding a 610 nm cutoff long-pass filter in the light path, resulted in a reasonably reversible sensor for both cases.

METHODS

Reagents. Silver nitrate (Aldrich, 99%), sodium citrate tribasic dihydrate (Aldrich, 99%), polyvinylpyrrolidone (PVP, *M*w 40K),

sodium borohydride (Aldrich, 99%), and L-arginine (Aldrich, 98%) were used as received. Millipore deionized water was used as solvent.

Synthesis of Silver Nanorods. Silver nanorods were synthesized following mainly the procedure developed by Kitaev *et al.*[18] Decahedral Ag nanoparticles were used as seeds. For their synthesis, a precursor solution of silver nanoparticles was first prepared using a mixture of 1.000 mL of 0.05 M sodium citrate, 0.060 mL of 0.05 M PVP, 0.100 mL of 0.005 M L-arginine, 0.400 mL of 0.005 M AgNO$_3$ and 14.0 mL of deionized water in a 20 mL vial. The solution was then reduced by adding 0.160 mL of 0.10 M NaBH$_4$. The resulting yellow solution was stirred for several minutes. To produce decahedra, a blue diode array lamp with $\lambda_{max} \approx 460$ nm with an exposure time of 10 h was used (LED spectrum Figure S4 in the Supporting Information). In the next step, 2 mL of the freshly prepared decahedral Ag seed solution were centrifuged to replace the supernatant with 1.0 mL of pure deionized water.

Once the decahedra seed solution was prepared, 1 mL of the purified decahedra solution, 2.0 mL of water, 0.400 mL of 0.05 M sodium citrate, and 0.066 mL of 0.05 M PVP were heated to 95 °C in a 20 mL vial in microwave oven at 90 W power. After temperature equilibration, 0.400 mL of silver nitrate (0.005 M) were added at once to produce rods with an aspect ratio up to 4−5 in high yield in 2−6 min of the reaction under 90 W microwave power.

Characterization. Transmission electron microscopy was performed using FEI Tecnai F30 and Phillips EM-420 microscopes. Nanoparticle solutions were deposited on a carbon-coated Formvar grid (Plano). Operating voltage was varied from 120 to 300 kV. The average size and standard deviation were determined from TEM images by averaging diameters of about 100 particles. Ensemble optical spectra were acquired with Ocean Optics USB 2000 spectrometer.

Single-Particle Microscopy. The single-particle spectroscopy was performed with a self-build microscopy setup employing a 2D piezo scanner. The setup shown in Figure 2 consists of a positioning stage (PI P-542.2CD Nanopositioning and Scanning Stage), microscope optics (Zeiss Achroplan Oil-Iris, 100×, NA = 0.7−1.25), an imaging spectrometer (Princeton Instruments/ACTON, SpectraPro 2300), and a CCD camera (Princeton Instruments, Pixis 400B). During a spectral scan, the sample is moved in steps of 1 μm along the *x*-axis. At each step, the spectrum of the particles in the center column is taken. The scan window width is adjusted to the step size to ensure gapless coverage of the scanned area.

Flow Cell. The glass capillary (Vitrotube W5010-100 by Vitrocom) is initially UV-irradiated for 15 min and left for another 15 min in the reactive atmosphere, then we attach thin polyethylene tubing using epoxy glue to construct the flow cell system. The flow cell is purged with 1% Helmanex solution for 24 h, and finally cleaned with hot deionized water for 1 h.

Supporting Information Available: Size distribution histograms and a table with size characteristics of the silver nanoparticles (Figure S1, Table S1), ensemble extinction spectrum of the measured gold NRs, the spectrum of the LED-lamp (Figure S4), a representative single-particle spectrum of silver NRs (Figure S5) and gold NRs (Figure S6). All measured single-particle sensitivity results are plotted in Figure S7. To compare the results with figure of merit sensitivity measures we included a plot of FOM and linewidth in Figure S8, stability measurements in pure water (Figure S9), and a graph comparing size and material dependent sensitivities obtained by MLWA calculations (Figure S10). We also present the derivation of the sensitivity formula. This material is available free of charge *via* the Internet at http://pubs.acs.org.

REFERENCES AND NOTES

1. Baciu, C. L.; Becker, J.; Janshoff, A.; Sönnichsen, C. Protein-Membrane Interaction Probed by Single Plasmonic Nanoparticles. *Nano Lett.* **2008**, *8*, 1724–1728.

2. Mayer, K. M.; Hao, F.; Lee, S.; Nordlander, P.; Hafner, J. H. A Single Molecule Immunoassay by Localized Surface Plasmon Resonance. *Nanotechnology* **2010**, *21*, 255503.

3. Wu, C. L.; Xu, Q. H. Stable and Functionable Mesoporous Silica-Coated Gold Nanorods as Sensitive Localized Surface Plasmon Resonance (LSPR) Nanosensors. *Langmuir* **2009**, *25*, 9441–9446.

4. Otte, M. A.; Sepulveda, B.; Ni, W. H.; Juste, J. P.; Liz-Marzan, L. M.; Lechuga, L. M. Identification of the Optimal Spectral Region for Plasmonic and Nanoplasmonic Sensing. *ACS Nano* **2010**, *4*, 349–357.

5. Kelly, K. L.; Coronado, E.; Zhao, L. L.; Schatz, G. C. The Optical Properties of Metal Nanoparticles: The Influence of Size, Shape, and Dielectric Environment. *J. Phys. Chem. B* **2003**, *107*, 668–677.

6. Becker, J.; Trügler, A.; Jakab, A.; Hohenester, U.; Sönnichsen, C. The Optimal Aspect Ratio of Gold Nanorods for Plasmonic Bio-sensing. *Plasmonics* **2010**, *5*, 161–167.

7. Khalavka, Y.; Becker, J.; Sönnichsen, C. Synthesis of Rod-Shaped Gold Nanorattles with Improved Plasmon Sensitivity and Catalytic Activity. *J. Am. Chem. Soc.* **2009**, *131*, 1871–1875.

8. Mahmoud, M. A.; El-Sayed, M. A. Gold Nanoframes: Very High Surface Plasmon Fields and Excellent Near-Infrared Sensors. *J. Am. Chem. Soc.* **2010**, *132*, 12704–12710.

9. Liz-Marzan, L. M. Tailoring Surface Plasmons through the Morphology and Assembly of Metal Nanoparticles. *Langmuir* **2006**, *22*, 32–41.

10. Wang, H. Y.; Reinhard, B. M. Monitoring Simultaneous Distance and Orientation Changes in Discrete Dimers of DNA Linked Gold Nanoparticles. *J. Phys. Chem. C* **2009**, *113*, 11215–11222.

11. Jain, P. K.; El-Sayed, M. A. Noble Metal Nanoparticle Pairs: Effect of Medium for Enhanced Nanosensing. *Nano Lett.* **2008**, *8*, 4347–4352.

12. Ringe, E.; McMahon, J. M.; Sohn, K.; Cobley, C.; Xia, Y. N.; Huang, J. X.; Schatz, G. C.; Marks, L. D.; Van Duyne, R. P. Unraveling the Effects of Size, Composition, and Substrate on the Localized Surface Plasmon Resonance Frequencies of Gold and Silver Nanocubes: A Systematic Single-Particle Approach. *J. Phys. Chem. C* **2010**, *114*, 12511–12516.

13. Wei, H.; Reyes-Coronado, A.; Nordlander, P.; Aizpurua, J.; Xu, H. X. Multipolar Plasmon Resonances in Individual Ag Nanorice. *ACS Nano* **2010**, *4*, 2649–2654.

14. Malinsky, M. D.; Kelly, K. L.; Schatz, G. C.; Van Duyne, R. P. Nanosphere Lithography: Effect of Substrate on the Localized Surface Plasmon Resonance Spectrum of Silver Nanoparticles. *J. Phys. Chem. B* **2001**, *105*, 2343–2350.

15. Haes, A. J.; Zou, S. L.; Schatz, G. C.; Van Duyne, R. P. Nanoscale Optical Biosensor: Short Range Distance Dependence of the Localized Surface Plasmon Resonance of Noble Metal Nanoparticles. *J. Phys. Chem. B* **2004**, *108*, 6961–6968.

16. Lee, K. S.; El-Sayed, M. A. Gold and Silver Nanoparticles in Sensing and Imaging: Sensitivity of Plasmon Response to Size, Shape, and Metal Composition. *J. Phys. Chem. B* **2006**, *110*, 19220–19225.

17. Meier, M.; Wokaun, A. Enhanced Fields on Large Metal Particles−Dynamic Depolarization. *Opt. Lett.* **1983**, *8*, 581–583.

18. Pietrobon, B.; McEachran, M.; Kitaev, V. Synthesis of Size-Controlled Faceted Pentagonal Silver Nanorods with Tunable Plasmonic Properties and Self-Assembly of These Nanorods. *ACS Nano* **2009**, *3*, 21–26.

19. Nikoobakht, B.; El-Sayed, M. A. Preparation and Growth Mechanism of Gold Nanorods (NRs) Using Seed-Mediated Growth Method. *Chem. Mater.* **2003**, *15*, 1957–1962.

20. Ni, W.; Kou, X.; Yang, Z.; Wang, J. F. Tailoring Longitudinal Surface Plasmon Wavelengths, Scattering and Absorption Cross Sections of Gold Nanorods. *ACS Nano* **2008**, *2*, 677–686.

21. Carbone, L.; Jakab, A.; Khalavka, Y.; Sönnichsen, C. Light-Controlled One-Sided Growth of Large Plasmonic Gold Domains Observed on the Single Particle Level. *Nano Lett.* **2009**, *9*, 3710–3714.

ARTICLE

22. Tsuji, T.; Okazaki, Y.; Higuchi, T.; Tsuji, M. Laser-Induced Morphology Changes of Silver Colloids Prepared by Laser Ablation in Water—Enhancement of Anisotropic Shape Conversions by Chloride Ions. *J. Photochem. Photobiol., A* **2006**, *183*, 297–303.
23. Sherry, L. J.; Chang, S. H.; Schatz, G. C.; Van Duyne, R. P.; Wiley, B. J.; Xia, Y. N. Localized Surface Plasmon Resonance Spectroscopy of Single Silver Nanocubes. *Nano Lett.* **2005**, *5*, 2034–2038.
24. Unger, A.; Kreiter, M. Analyzing the Performance of Plasmonic Resonators for Dielectric Sensing. *J. Phys. Chem. C* **2009**, *113*, 12243–12251.
25. Hohenester, U.; Krenn, J. Surface Plasmon Resonances of Single and Coupled Metallic Nanoparticles: A Boundary Integral Method Approach. *Phys. Rev. B* **2005**, *72*, 195429.
26. Tang, Y.; Ouyang, M. Tailoring Properties and Functionalities of Metal Nanoparticles Through Crystallinity Engineering. *Nat. Mater.* **2007**, *6*, 754–759.
27. Miller, M. M.; Lazarides, A. A. Sensitivity of Metal Nanoparticle Surface Plasmon Resonance to the Dielectric Environment. *J. Phys. Chem. B* **2005**, *109*, 21556–21565.
28. Jiang, X. C.; Yu, A. B. Silver Nanoplates: A Highly Sensitive Material Toward Inorganic Anions. *Langmuir* **2008**, *24*, 4300–4309.
29. Cathcart, N.; Frank, A. J.; Kitaev, V. Silver Nanoparticles with Planar Twinned Defects: Effect of Halides for Precise Tuning of Plasmon Resonance Maxima from 400 to >900 nm. *Chem. Commun.* **2009**, 7170–7172.
30. Jin, R. C.; Cao, Y. W.; Mirkin, C. A.; Kelly, K. L.; Schatz, G. C.; Zheng, J. G. Photoinduced Conversion of Silver Nanospheres to Nanoprisms. *Science* **2001**, *294*, 1901–1903.
31. Mock, J. J.; Barbic, M.; Smith, D. R.; Schultz, D. A.; Schultz, S. Shape Effects in Plasmon Resonance of Individual Colloidal Silver Nanoparticles. *J. Chem. Phys.* **2002**, *116*, 6755–6759.
32. Plech, A.; Kurbitz, S.; Berg, K. J.; Graener, H.; Berg, G.; Gresillon, S.; Kaempfe, M.; Feldmann, J.; Wulff, M.; von Plessen, G. Time-Resolved X-ray Diffraction on Laser-Excited Metal Nanoparticles. *Europhys. Lett.* **2003**, *61*, 762–768.